Chain Dynamics and the Simulation of Electron Spin Resonance Spectra from Oriented Phospholipid Membranes

Roberta Cassol,[†,‡] Ming-Tao Ge,[†] Alberta Ferrarini,[‡] and Jack H. Freed*[,†]

Department of Chemistry, Cornell University, Ithaca, New York 14853, and Department of Physical Chemistry, University of Padua, Padua, Italy 35131

Received: January 3, 1997; In Final Form: April 3, 1997[⊗]

A model previously developed for describing the dynamics of flexible alkyl chains that is based on Flory's rotational isomeric state approximation is adapted and applied to the analysis of electron spin resonance (ESR) spectra obtained from a phospholipid spin label in a macroscopically aligned phospholipid membrane. In this model, rotation around each C−C bond of the labeled alkyl chain is characterized by three inequivalent minima, with one end of the chain fixed to mimic the phospholipid headgroup, and with the dynamic effects of the nitroxide label explicitly included. This model is integrated with that for the overall rotation of the phospholipid in the mean orientational potential of the aligned membrane, and it is incorporated into the stochastic Liouville equation which describes the ESR line shape in the presence of these dynamic processes. The analysis is simplified by introducing the fact that the relatively rapid internal modes of motion can be treated by motional narrowing theory and a time scale separation can be made with respect to the much slower overall motions of the phospholipid. A series of ESR spectra from the spin label 16-PC in the lipid dimyristoylphosphatidylcholine were obtained over a range of temperatures (35−65 °C) in the L_α phase for various orientations of the normal to the bilayer plane relative to the magnetic field. Very good agreement with experiment is obtained from this model by using least squares fitting procedures for the overall motional dynamics. One finds an order parameter of $\langle D^2_{00}\rangle$ that is constant throughout the phase and the perpendicular component for rotational diffusion, $R_\perp$, that ranges from about $1-3 \times 10^7 s^{-1}$ (which corresponds to the ESR slow motional regime). Fits to the ESR spectra were also obtained from a simple but standard model wherein a single overall rotational diffusion tensor is used to describe the combined effects of internal and overall dynamics. These fits were almost as good, but they lead to a much larger $R_\perp \approx 3-6 \times 10^8\ s^{-1}$ and a smaller $\langle D^2_{00}\rangle = 0.1$, since these parameters now include the composite effects of both types of processes. New ESR experiments are proposed to provide more critical tests of these models.

1. Introduction

Electron spin resonance (ESR) has over the years proved to be very useful in providing insight into the dynamic molecular structure of phospholipid membranes by the utilization of appropriate spin labels.[1,2] In particular, by means of careful line shape analysis, one may obtain the details of the motions.[3−7] The usual procedure is to use a simple model, consistent with the resolution of the continuous wave (cw) ESR experiment, based upon a Smoluchowski equation representing the anisotropic rotational diffusion of the labeled lipid (or cholesterol) molecule in the mean orienting potential provided by the other lipid molecules in the membrane. This is meant as an approximation to the actual, more complex dynamical behavior,[1] which would require a much more sophisticated analysis of the complex internal modes of chain dynamics as well as the overall motion of the lipid molecule.

In the last several years,[8,9] a model has been developed that is suitable to describe the kinetics of conformational transitions in flexible alkyl chains, and it has recently been adapted to a nitroxide spin label, linked by alkyl chains to a larger molecule (e.g. a polypeptide) in isotropic solution.[10] In the present work it is extended to apply to oriented phases in a way that is related to its previous application to the L_α phase of phospholipid membranes for the interpretation of selective ^{13}C or ^2H NMR relaxation[9] at the various carbon positions along the alkyl chains. The new features required for ESR studies of nitroxide labels are (1) the explicit inclusion of the nitroxide moiety attached to the chain, and (2) the recognition that for the faster time scales of ESR vs NMR the overall motion of the phospholipid is likely to be in the slow motional regime, necessitating the use of the stochastic Liouville equation (SLE).[3,4] We discuss these matters in more detail below.

Specifically, we have considered ESR spectra of 16-PC in oriented membranes of DMPC (PC = phosphatidylcholine, DMPC = dimyristoylphosphatidylcholine)[11] (Figure 1) at different temperatures and orientations of the magnetic field with respect to the director, i.e. the direction of preferential alignment of the lipid molecules.

In the most detailed model we utilize to analyze these results, the two kinds of motions with different time scales are the fast conformational motion of the internal degrees of freedom of the chain, with frequencies of about $10^{10}\ s^{-1}$, and the slower motion of the whole phospholipid molecule characterized by slower rates of relaxation. In general, the ESR spectral shape is strongly influenced by fluctuations in the magnetic interactions, which occur in the fluid system because of these various diffusive motions. The fluctuations in the magnetic interactions may be characterized by the mean square value, Δ^2, of the interaction and by the characteristic time, τ, of the fluctuations. We can distinguish two limiting regimes: (a) the fast motional regime defined by the expression $\Delta^2\tau^2 < 1$ and (b) the slow motional regime defined by the condition $\Delta^2\tau^2 > 1$. In case b the spin degrees of freedom and the molecular dynamics are

[†] Cornell University.
[‡] University of Padua.
[⊗] Abstract published in *Advance ACS Abstracts,* September 15, 1997.

S1089-5647(97)00071-0 CCC: $14.00

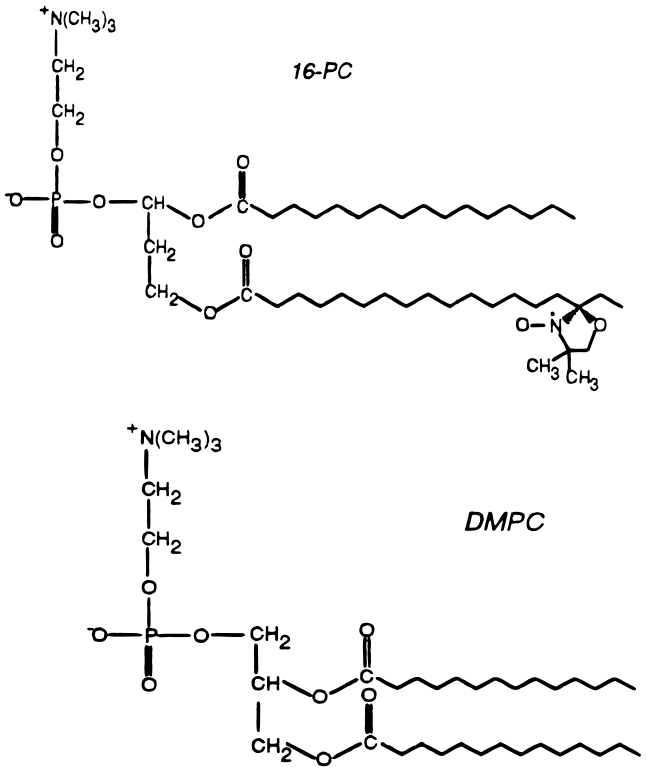

Figure 1. Structures of spin-labeled phosphatidylcholine (16-PC) and dimyristoylphosphatidylcholine (DMPC).

strongly coupled. More detailed information on the molecular dynamics can be obtained from spectra in the slow motional regime, which, however, requires the more complex theoretical analysis of the SLE, as noted above.

In this paper we actually consider three different approaches involving varying levels of approximation, and they are described in the following sections. The first model is the conventional one.[1−4] It considers a nitroxide label as simply rotating in a liquid crystalline environment with a single "effective" diffusion tensor that is a simple approximation to the internal motions of the aliphatic chain as well as to the overall motion of the phospholipid molecule. In the second approach, the internal dynamics of the chain is treated in detail in terms of the conformational transitions described by the rotational isomeric state model[8,12] whereas the overall motion of the phospholipid molecule is assumed to be so slow that it only produces a static distribution of molecular orientations with respect to the macroscopic orienting potential. Thus, the spectra have been calculated by averaging over such a distribution. In the last and most complete model, both the slow overall rotations of the phospholipid molecule and the faster conformational transitions of the chain are explicitly taken into account. We consider the extent to which these models are able to fit the experimental results and the resultant implications for studying the complex dynamics.

2. Theory: Simulation of the ESR Spectra

The spin Hamiltonian for nitroxide radicals, written as the contraction of irreducible spherical tensors, can be expressed as the sum of two terms, one independent of and the other dependent on the orientation and conformation of the molecule, given by $\mathbf{\Theta}$

$$\hat{H}(\mathbf{\Theta}) = \hat{H}_0 + \hat{H}_1(\mathbf{\Theta}) = \sum_{\mu} F_{\mu}^{(00)*} T_{\mu}^{(00)} + \sum_{\mu m} F_{\mu}^{(2m)*} T_{\mu}^{(2m)} \quad (1)$$

where μ indicates the kind of magnetic interaction, in our case the Zeeman and hyperfine interactions, and $F_{\mu}^{(lm)}$ and $T_{\mu}^{(lm)}$ are the irreducible spherical components of the magnetic tensors and the spin operators, respectively.[1,3,4] The nuclear Zeeman interaction need not be included to a good approximation, so the quantization axis of the nuclear spin is determined by the hyperfine term for which the nonsecular terms are neglected based on the limit, fulfilled in this work, $\omega^2_0\tau^2 \gg 1$ (where ω_0 is the ESR resonant frequency).

It is convenient to express the spin operators in a laboratory frame having its Z_L axis parallel to the static magnetic field B_0, and the magnetic tensors **g** and **A** in their principal axis systems M_g and M_A, which in general need not coincide. Thus, the rotation from the laboratory frame M_L to the frames M_g and M_A can be decomposed in terms of the the following sequence of rotations

$$M_L \xrightarrow{\mathbf{\Psi}} M_d \xrightarrow{\mathbf{\Omega}} M_R \xrightarrow{\mathbf{\Phi}} M_g \xrightarrow{\chi} M_A \quad (2)$$

where M_d is the director frame, with the Z_d axis along the local director, i.e. the preferred axis of alignment of the phospholipid molecule, and M_R is the principal axis system of the rotational diffusion tensor of the molecule. Usually the set of angles $\boldsymbol{\chi}$ is taken to be {0,0,0} corresponding to a common axis system for **g** and **A**, so we will omit it in the next expressions. According to the usual convention, the reference system for M_g (and M_A) is chosen with the z axis parallel to the p_z orbital of the nitrogen atom and the x axis along the N−O bond.

Thus we have the following general expressions for the tensors in the laboratory system

$$F_{g,L}^{(2m)} = \sum_{rqp} D_{mr}^{2}*(\mathbf{\Psi}) D_{rq}^{2}*(\mathbf{\Omega}) D_{qp}^{2}*(\mathbf{\Phi}) F_{g}^{(2p)} \quad (3)$$

$$F_{A,L}^{(2m)} = \sum_{rqp} D_{mr}^{2}*(\mathbf{\Psi}) D_{rq}^{2}*(\mathbf{\Omega}) D_{qp}^{2}*(\mathbf{\Phi}) F_{A}^{(2p)} \quad (4)$$

where D^{j}_{mk} are the Wigner rotation matrix components. Substituting eqs 3 and 4 into eq 1 we obtain

$$\hat{H}_1(\mathbf{\Theta}) = \sum_{rqp} D_{0r}^{2}*(\mathbf{\Psi}) D_{rq}^{2}*(\mathbf{\Omega}) D_{qp}^{2}*(\mathbf{\Phi}) F_{g}^{(2p)} T_{g}^{(20)} + \sum_{mrqp} D_{mr}^{2}*(\mathbf{\Psi}) D_{rq}^{2}*(\mathbf{\Omega}) D_{qp}^{2}*(\mathbf{\Phi}) F_{A}^{(2p)} T_{A}^{(2m)} \quad (5)$$

Following linear response theory[3] the intensity of the absorbed radiation is proportional to the imaginary part of the magnetic susceptibility, χ''

$$\chi''(\pm\omega) = \frac{N\gamma_e^2\omega}{2Nk_BT} \mathrm{Tr}_S \overline{\{S_x\, S_x(\pm\omega)\}} \quad (6)$$

where Tr_S denotes a trace over the spin degrees of freedom and the overbar implies the statistical average over the spatial variables of the paramagnetic system, while $\{S_xS_x(\pm\omega)\}$ is the Fourier−Laplace transform of the correlation function for the operator S_x associated with the component of the magnetization parallel to the x axis. The time evolution of the correlation function is determined by the dynamics of the system.

2.1. Model A: Stochastic Liouville Equation for a Simple Nitroxide. The spectrum is simulated by solving the stochastic Liouville equation for the temporal evolution of the density matrix $\boldsymbol{\rho}(\mathbf{\Omega},t)$, $\mathbf{\Omega}$ representing the orientational degrees of freedom of the nitroxide spin label[3,4]

$$\frac{\partial \boldsymbol{\rho}(\mathbf{\Omega},t)}{\partial t} = -i\mathbf{L}(\mathbf{\Omega})\, \boldsymbol{\rho}(\mathbf{\Omega},t) - \mathbf{\Gamma}(\mathbf{\Omega})\, \boldsymbol{\rho}(\mathbf{\Omega},t) \quad (7)$$

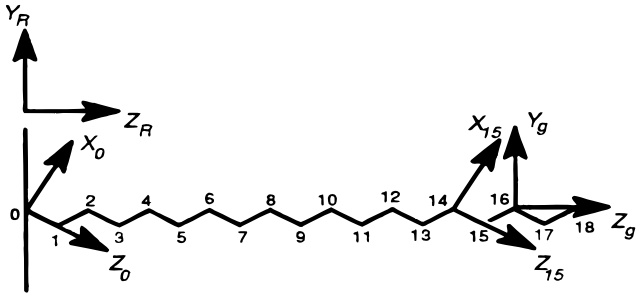

Figure 2. Model system for spin-labeled chain of 16-PC. The principal axes of M_R, M_0, M_{15}, and M_g (cf. eq 11) are shown.

where **L** is the Liouville superoperator associated with the spin Hamiltonian of eq 1 and $\mathbf{\Gamma}(\mathbf{\Omega})$ is the diffusion operator for rotation in the presence of an orienting potential (i.e. a Smoluchowski operator), whose symmetrized form is

$$\tilde{\mathbf{\Gamma}}(\mathbf{\Omega}) = \left(\hat{L} - \frac{(\hat{L}U(\mathbf{\Omega}))}{2k_BT}\right)\boldsymbol{R}\left(\hat{L} + \frac{(\hat{L}U(\mathbf{\Omega}))}{2k_BT}\right) \quad (8)$$

$\hat{L}$ is the operator generating infinitesimal rotations of the diffusive system with respect to the director frame, **R** is the rotational diffusion tensor and $U(\mathbf{\Omega})$ is the orienting potential acting on the spin label. The expansion in Wigner functions, $D^L_{0m}(\mathbf{\Omega})$, appropriate for a uniaxial environment, is usually truncated at the second-rank term, and the following expression is obtained:

$$U(\mathbf{\Omega}) = -k_BT\{C_{20}D^2_{00}(\mathbf{\Omega}) + C_{22}[D^2_{02}(\mathbf{\Omega}) + D^2_{0-2}(\mathbf{\Omega})]\} \quad (9)$$

The spectral density for the *x* component of the magnetization is then given by[3]

$$\mathrm{Tr}_s\, \overline{S_jS_j(\pm\omega,\mathbf{\Omega})} = \langle P_0^{1/2}S_j|[\mathrm{i}(\omega\mathbf{I} - \mathbf{L}) + \tilde{\mathbf{\Gamma}}^\dagger]^{-1}|P_0^{1/2}S_j\rangle \quad (10)$$

[Note that in eq 10 there is an implicit dependence upon Ψ that is not displayed.]

The numerical procedure for the calculation of the spectral density is based on an expansion in the direct product space of Wigner functions and the space of spin transitions. Then, transforming the matrix $[\mathrm{i}(\omega\,\mathbf{I} - \mathbf{L}) + \tilde{\mathbf{\Gamma}}^\dagger]^{-1}$ to tridiagonal form by means of an efficient algorithm, such as the conjugate gradient method, the spectral densities are obtained with the continued fraction method.[4] This is a general approach, which can be used without restrictions on the motional regime, and in particular it can be employed for the analysis of slow motional spectra.[3]

2.2. Model B: Redfield Approximation for the Chain Dynamics. In this model the internal rotations are taken explicitly into account. Thus the transformations from the M_R reference system to the magnetic frame M_g (coincident with M_A) depend on the torsional angles in the 16-PC chain bearing the nitroxide spin label.

$$M_L \xrightarrow{\mathbf{\Psi}} M_d \xrightarrow{\mathbf{\Omega}} M_R \xrightarrow{\mathbf{\Omega}_4} M_0 \xrightarrow{\omega_1} \ldots \xrightarrow{\omega_{15}} M_{15} \xrightarrow{\mathbf{\Omega}_5} M_g \quad (11)$$

The Euler angle $\mathbf{\Omega}_4$ transforms from the diffusive system M_R to the system on the first or uppermost C−C bond of the aliphatic chain and is equal to the set of angles {180°,35.3°,180°}. This means that the *z* axis of M_R is parallel to the all-trans axis of the chain. The reference systems $\{M_0, \ldots, M_{15}\}$ are defined with respect to all the C−C bonds of the chain up to the atom linked to the nitroxide moiety. The angle $\mathbf{\Omega}_5$ rotates from this last bond to the magnetic system of the **g** tensor. Thus the sequence $\mathbf{\Omega}_4$, $\boldsymbol{\omega}_1$, ..., $\boldsymbol{\omega}_{15}$, $\mathbf{\Omega}_5$ replaces the simple Euler angle $\mathbf{\Phi}$ in eq 2. This is illustrated in part in Figure 2.

Since the conformational motions are fast on the ESR time scale, the simulation of the spectra does not require the full solution of the stochastic Liouville equation for the torsional degrees of freedom coupled to the spin variables. Instead a simpler approach can be used, based on the Redfield, or motional narrowing, approximation.[13,14] Thus, a spectrum is given by three lines whose position is determined by the static spin Hamiltonian, partially averaged by the chain dynamics.[10] It can be written as

$$\hat{H}_0 + \overline{\hat{H}_1} = \hat{H}_0 + \sum_{rq} D^2_{0r}{}^*(\mathbf{\Psi})D^2_{rq}{}^*(\mathbf{\Omega})\,\overline{F^{(2q)}_{g,R}}\,T^{20}_g + \sum_{mrq} D^2_{mr}{}^*(\mathbf{\Psi})D^2_{rq}{}^*(\mathbf{\Omega})\,\overline{F^{(2q)}_{A,R}}\,T^{2m}_M \quad (12)$$

where the overbar denotes the average over the distribution in torsional angles, and

$$\overline{F^{(2q)}_{g,R}} = \sum_p \overline{D^2_{qp}{}^*(\mathbf{\Phi})}F^{(2p)}_g \quad (13)$$

$$\overline{F^{(2q)}_{A,R}} = \sum_p \overline{D^2_{qp}{}^*(\mathbf{\Phi})}F^{(2p)}_A \quad (14)$$

The line width is given by Redfield theory[13,14]

$$(T_{2,m})^{-1} = A(\mathbf{\Psi},\mathbf{\Omega}) + B(\mathbf{\Psi},\mathbf{\Omega})m + C(\mathbf{\Psi},\mathbf{\Omega})m^2 \quad (15)$$

where $m = 0,\pm1$ indicates the nuclear spin states, and the coefficients $A(\mathbf{\Psi},\mathbf{\Omega})$, $B(\mathbf{\Psi},\mathbf{\Omega})$, $C(\mathbf{\Psi},\mathbf{\Omega})$ arise from the spectral densities for the magnetic tensors, $J^{(\mu\mu')}_m$,[10] and they depend on both $\mathbf{\Psi}$ and $\mathbf{\Omega}$.

Since we are neglecting the nonsecular contributions of the relaxation matrix, only the zero-frequency spectral densities are needed

$$J^{(\mu\mu')}_m = {}^1/_2\int_{-\infty}^{\infty}\overline{F^{(2m)}_\mu(0)\,F^{(2m)}_\mu(t)^*}\,\mathrm{d}t \quad (16)$$

$$A(\mathbf{\Psi},\mathbf{\Omega}) = {}^2/_3J^{gg}_0 + {}^1/_2J^{AA}_1 \quad (17)$$

$$B(\mathbf{\Psi},\mathbf{\Omega}) = {}^2/_3(J^{gA}_0 + J^{Ag}_0) = {}^4/_3J^{gA}_0 \quad (18)$$

$$C(\mathbf{\Psi},\mathbf{\Omega}) = {}^2/_3J^{AA}_0 - {}^1/_4J^{AA}_1 \quad (19)$$

where the explicit forms of the $J^{(\mu\mu')}_m$ are

$$J^{gg}_0 = \sum_{r_1q_1p_1r_2q_2p_2} F^{(2p_1)}_g F^{(2p_2)}_g{}^* j_{q_1p_1q_2p_2} D^2_{0r_1}{}^*(\mathbf{\Psi})D^2_{0r_2}(\mathbf{\Psi}) \times D^2_{r_1q_1}{}^*(\mathbf{\Omega})D^2_{r_2q_2}(\mathbf{\Omega}) \quad (20)$$

$$J^{gA}_0 = \sum_{r_1q_1p_1r_2q_2p_2} F^{(2p_1)}_g F^{(2p_2)}_A{}^* j_{q_1p_1q_2p_2} D^2_{0r_1}(\mathbf{\Psi})^* D^2_{0r_2}(\mathbf{\Psi}) \times D^2_{r_1q_1}{}^*(\mathbf{\Omega})D^2_{r_2q_2}(\mathbf{\Omega}) \quad (21)$$

$$J^{AA}_m = \sum_{r_1q_1p_1r_2q_2p_2} F^{(2p_1)}_A F^{(2p_2)}_A{}^* j_{q_1p_1q_2p_2} D^2_{mr_1}{}^*(\mathbf{\Psi})D^2_{mr_2}(\mathbf{\Psi}) \times D^2_{r_1q_1}{}^*(\mathbf{\Omega})D^2_{r_2q_2}(\mathbf{\Omega}) \quad (22)$$

and the $j_{q_1p_1q_2p_2}$ are the zero-frequency spectral densities which are the Fourier−Laplace transforms of the correlation functions of the appropriate Wigner rotation matrix components over the internal chain dynamics.[9,10,15]

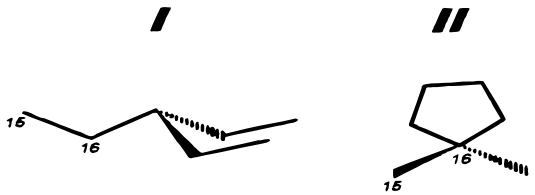

Figure 3. Models for nitroxide moiety attached to position 16: type I, extended form; type II, pentagon (cf. text).

The final expression for the ESR line shape is

$$I(\omega,\mathbf{\Omega},\mathbf{\Psi}) = \frac{1}{\pi}\sum_{m=0,\pm1} Re\left[i(\omega - \omega_m(\mathbf{\Omega},\mathbf{\Psi})) + \frac{1}{T_{2,m}}(\mathbf{\Omega},\mathbf{\Psi})\right]^{-1} \tag{23}$$

where $\omega_m(\mathbf{\Omega},\mathbf{\Psi})$ is the resonance frequency obtained by the diagonalization of the partially averaged Hamiltonian.

The above expressions display the dependence of the spectrum upon $\mathbf{\Omega}$, the molecular orientation with respect to the director. The phospholipid chains in a bilayer are not perfectly aligned with respect to the director. If the overall reorientation is very slow on the ESR time scale, the spectrum can be obtained as a sum of contributions from each molecular orientation

$$I(\omega) = \frac{1}{\pi} Re \sum_{m=0,\pm1} \int \mathrm{d}\beta \sin\beta\, P(\beta)[i(\omega - \omega_m(\beta)) + T_{2,m}^{-1}]^{-1} \tag{24}$$

where β is the angle between the director and the all-trans axis of the chain, and $P(\beta)$ is the orientational distribution function, which in its simplest form may be taken as

$$P(\mathbf{\Omega}) \propto \mathrm{e}^{-\lambda \sin 2\beta} \tag{25}$$

The partially averaged tensors, eqs 13 and 14, and the spectral densities, eqs 20−22, can be evaluated given the distribution of the torsional angles as well as a model for the chain dynamics.

2.2.1. Chain Model. The model system is an aliphatic chain with 15 torsional degrees of freedom and a spin probe linked to carbon 16, sketched in Figure 2. The zero position corresponds to the chain oxygen atom in Figure 1. For the evaluation of steric and friction effects, the chain is considered as an assembly of 18 interlocking van der Waals spheres centered at the carbon positions and corresponding to the methylene groups and to the terminal methyl group.

The spin probe is simulated by four atoms linked to the chain in such a way as to form a pentagon (cf. Figure 3 type II). The steric effects are evaluated, as for the chain, by including four van der Waals spheres. We also performed the calculation for another shape of the spin label (cf. Figure 3 type I), and we obtained almost the same results, showing that the global volume is more important than the actual shape.

The rotation around each C−C bond is subjected to a torsional potential characterized by three inequivalent minima corresponding to the gauche−, trans, and gauche+ states. The C_1−C_2 bond is an exception. It is given by a potential with three equivalent minima in order to mimic the effect of the phospholipid headgroup.[9] Due to the adoption of the rotational isomeric state (RIS)[12] approximation only a discrete number of states, corresponding to the minima of the torsional potential, are considered. Thus the number of possible conformers is 3.[15] However, this number is greatly reduced because of excluded volume effects of the methylenes of the chain with each other and with the polar headgroup. These effects are taken into account by rejecting all the conformers with g+g− sequences and with at least two atoms closer than a minimum approach distance equal to 2 Å. In addition, as a consequence of the bilayer structure, those folded conformations with atoms extending beyond a surface perpendicular to the all-trans chain and passing through the oxygen atom are rejected. The final number of chain conformers is about 6.6×10^5.

The orientational order acting on the chain in the bilayer environment is introduced into the model with an orienting potential acting on each chord of the angle $C_{i-1}C_iC_{i+1}$, according to the Marcelja model:[16]

$$U_i^{or}(\cos\theta_i)/k_\mathrm{B}T = \epsilon\, P_2(\cos\theta_i) \tag{26}$$

Here θ_i defines the angle between the ith chord and the all-trans axis, and ϵ is the strength of the interaction potential in units of $k_\mathrm{B}T$.

Static properties are evaluated by averaging over the RIS conformers; thus for a generic function of the torsional angles $f(\mathbf{\Phi})$ we can write

$$\langle f\rangle \equiv \bar{f} = \sum_I f_I P_I \tag{27}$$

where f_I is the value of the function for the Ith RIS conformer and P_I is the corresponding statistical weight defined as

$$P_I = \exp(-U_I/k_\mathrm{B}T)/\sum_J \exp(-U_J/k_\mathrm{B}T) \tag{28}$$

The potential acting on the Ith conformer with n_g gauche dihedral angles is given by

$$U_I = \sum_i U_i^{or} + n_\mathrm{g}E_\mathrm{g} \tag{29}$$

The first term is the sum of the orienting potentials acting on the various chain segments, while the second is the torsional potential, simply written by adding a contribution E_g for each gauche state.

Dynamical properties are calculated by employing an extension of the RIS model to the time domain, which describes the conformational dynamics in terms of $t \rightleftharpoons g$ transitions.[8] The transition rates are derived by generalizing the one-dimensional Kramers result for overdamped regimes,[17] to the multidimensional case, according to a procedure developed by Langer.[18] The model has been presented and discussed elsewhere.[8,9] Therefore we shall not deal with the details in the present work. However, it is worth mentioning that, according to the model, the transition rate has to be evaluated for each conformational jump, since it depends on both the energetics and the friction characterizing the initial and the final conformation. Only single-bond transitions are considered, multiple transitions being neglected because of their unfavorable activation energy. However, the cooperative motion of segments near the bond undergoing the conformational transition, required in order to minimize the frictional torques, is also taken into account by the model. Another important feature of the model is that all properties can be evaluated as functions of a few well-defined parameters at a molecular level. In addition to the energy contribution E_g defined above, we note that a parameter, ρ, giving the ratio of the saddle point curvatures of the potential for the reactive and the nonreactive modes, and the scaling frequency, w, which can be related to the butane $g \rightarrow t$ isomerization rate,[8,9] are needed.

2.3. Model C: Stochastic Liouville Equation and Redfield Approximation. This model explicitly takes into account both the conformational motions and the overall rotations of the molecule. Thus we regard it as the most realistic. It utilizes the same analysis for the conformational motions (cf. eqs 12−22 and eqs 26−29) as was used in model B. Thus, we continue

to assume that a fast motional treatment applies to these conformational motions. However, instead of the simplifying assumption of extremely slow overall reorientation, which led to a static distribution of molecular orientations expressed by eqs 24 and 25, we allow the molecular orientations, $\mathbf{\Omega}$, to obey a Smoluchowski diffusion equation given by eq 8. Since, in general, this is a slow process, we must use a stochastic Liouville equation (cf. eq 7 for model A) that is appropriate for the combined processes of fast conformational and slow overall rotations.

To accomplish this we utilize a SLE with a density matrix which depends explicitly on the orientational degrees of freedom of the phospholipid molecule, $\mathbf{\Omega}$, but is averaged over the torsional angles of the chain, Φ. That is, a static Hamiltonian partially averaged by the chain dynamics (cf. eqs 12−14) is used. Also we use the diagonal matrix $\mathbf{T}_2^{-1}$ whose elements are given by eq 15. These elements are the $\mathbf{\Omega}$- and $\mathbf{\Psi}$-dependent line widths, i.e. they correspond to the residual line broadening from the rapid conformational motions, which depends on the instantaneous orientation $\mathbf{\Omega}$ of the phospholipid and the director tilt $\mathbf{\Psi}$. Then this $\mathbf{T}_2^{-1}$ is added to the diffusion operator $\mathbf{\Gamma}(\mathbf{\Omega})$ of eq 7, which accounts for the rotational motion of the whole molecule in a uniaxial environment, to yield

$$\frac{\partial \boldsymbol{\rho}(\mathbf{\Omega},t)}{\partial t} = -\mathrm{i}\,\overline{\mathbf{L}(\mathbf{\Omega})}\,\boldsymbol{\rho}(\mathbf{\Omega},t) - [\mathbf{T}_2^{-1}(\mathbf{\Omega}) + \mathbf{\Gamma}(\mathbf{\Omega})]\boldsymbol{\rho}(\mathbf{\Omega},t)$$

$$\equiv \mathbf{A}(\mathbf{\Omega})\,\boldsymbol{\rho}(\mathbf{\Omega},t) \qquad (30)$$

where $\overline{\mathbf{L}(\mathbf{\Omega})}$ is the Liouville superoperator associated with the partially averaged spin Hamiltonian of eq 12. (For convenience, we do not display the dependence on $\mathbf{\Psi}$ of these terms.)

As in the case of model A, the procedure adopted for the calculation to obtain the ESR spectra requires the expansion of the stochastic Liouville operator, $\mathbf{A}(\mathbf{\Omega})$ in a basis of orthonormal functions of $\mathbf{\Omega}$. Note that in the limit of very slow overall reorientation, model C becomes just model B.

In the past, a similar approach was proposed to obtain the ESR spectra of nitroxide spin labels linked by alkyl chains to macromolecules, but in that context a random or strong jump model was assumed for the overall motion superimposed on the conformational transitions, in place of rotational diffusion, and the medium was taken to be isotropic.[10]

3. Results

3.1. Experimental Spectra. ESR spectra of 16-PC in aligned DMPC membranes which have been hydrated in 100% humidity[6,7,11] have been obtained at the following temperatures: 35, 40, 45, 50, 55, 60, 65 °C at four different orientations of the static magnetic field with respect to the director: $\mathbf{\Psi}$ = 0, 30, 60, 90 °. They may be seen in Figures 4 and 5 for 35° and 55°, respectively.

The magnetic tensors were obtained from the analysis of rigid limit spectra that were obtained from the aligned membrane at −135 °C.[19] They are g_{xx}, g_{yy}, g_{zz} = 2.0089, 2.0058, 2.0021 and A_{xx}, A_{yy}, A_{zz} = 5, 5, 33.2 G. Note that the magnetic principal axes have the x axis along the nitroxide N−O bond, the z axis is along the 2p orbital of the nitrogen, and the y axis is perpendicular to the other two.

In the following sections we discuss the simulations performed with the three models.

3.2. Model A. The spectra were analyzed utilizing the ESR slow motional spectral calculation program[4] with a modified Levenberg−Marquardt nonlinear least-squares minimization algorithm.[7]

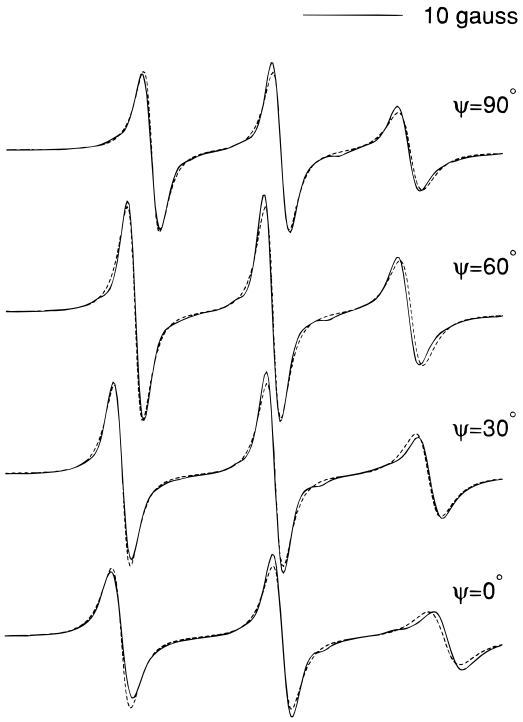

Figure 4. Experimental spectra obtained at 35 °C for tilt angles of 90°, 60°, 30°, and 0° shown by solid lines. Dashed lines show best fits to model A.

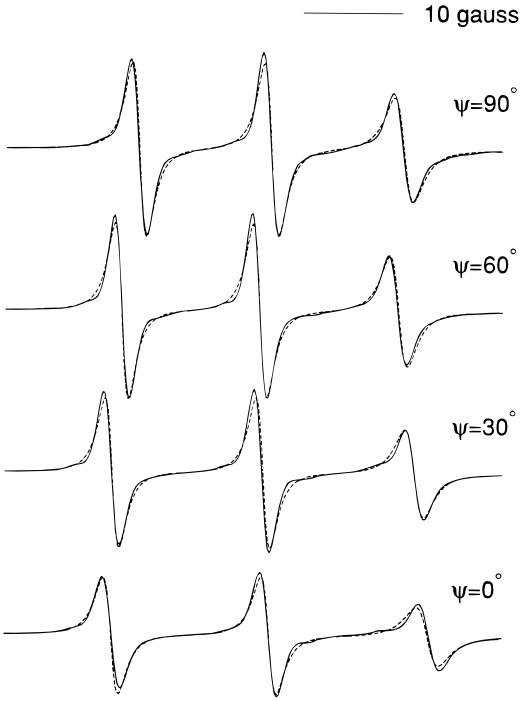

Figure 5. Experimental spectra obtained at 55 °C for tilt angles of 90°, 60°, 30°, and 0° shown by solid lines. Dashed lines show best fits to model A.

We performed the fits by varying the following parameters of the system:

(1) The parallel and perpendicular components of the diffusion tensor, $\mathbf{R}_\parallel$ and $\mathbf{R}_\perp$ (s^{-1}), characterizing the rotational dynamics of the spin label were varied; the ratio $N \equiv R_\parallel/R_\perp$ was taken to be constant and equal to 4 since the simulations were not sensitive to N. Following the usual procedure, the magnetic z axis was taken as parallel to the principal axis of diffusion.[5−7,11]

(2) The coefficient C_{20} which gives the strength of the orienting potential and which yields the order parameter

TABLE 1: Best Fitting Parameters for the ESR Spectra of 16-PC in Aligned Membranes of DMPC Using Model A

T (°C)	$\log(R_\perp)$	$\log(R_\parallel)$	C_{20}	$\langle D^2_{00}\rangle$
		0° Tilt Angle		
35	8.55	9.05	0.54	0.12
40	8.64	9.14	0.49	0.10
45	8.71	9.22	0.48	0.10
50	8.77	9.27	0.50	0.10
55	8.81	9.31	0.46	0.10
60	8.87	9.35	0.45	0.10
65	8.90	9.40	0.45	0.10
		30° Tilt Angle		
35	8.60	9.20	0.51	0.11
40	8.68	9.28	0.48	0.10
45	8.76	9.36	0.45	0.10
50	8.81	9.41	0.44	0.10
55	8.86	9.46	0.44	0.09
60	8.91	9.32	0.44	0.09
65	8.90	9.60	0.43	0.09
		60° Tilt Angle		
35	8.62	9.22	0.53	0.23
40	8.69	9.29	0.49	0.10
45	8.75	9.35	0.46	0.13
50	8.84	9.44	0.46	0.10
55	8.90	9.50	0.44	0.10
60	8.96	9.56	0.44	0.10
65	9.00	9.60	0.42	0.09
		90° Tilt Angle		
35	8.54	9.14	0.55	0.12
40	8.65	9.25	0.50	0.11
45	8.71	9.31	0.44	0.10
50	8.75	9.35	0.44	0.10
55	8.78	9.38	0.41	0.09
60	8.85	9.45	0.42	0.09
65	8.9	9.5	0.38	0.08

$\langle D^2_{00}\rangle$ was varied. (Note $D^2_{00}(\beta) = (3\cos^2\beta - 1)/2$ where β is the angle between the symmetry axis of the probe and the director.)

(3) The set of angles $\mathbf{\Phi}$ is taken equal to zero.

(4) In some preliminary simulations we found that varying the coefficient C_{22} resulted in negligible effects. Therefore, in the final simulations it was taken as equal to zero in order to reduce the number of fitting parameters. This is equivalent to assuming that the spin label tends to orient with the z axis of the magnetic system along the director, without any preference for the orientation of the x and y axis.

In Table 1 the fitting parameters are reported for the simulations of the spectra at all the temperatures and orientations of the director with respect to the magnetic field.[20] The rather good spectral fits are shown in Figures 4 and 5.

The diffusion tensor $\mathbf{R}$ is large because it must take into account not only the slow motion of the phospholipid molecule, but also the fast motion of the internal degrees of freedom of the aliphatic chain. For the same reason, the order parameter $\langle D^2_{00}\rangle$ has low values. In fact it reflects the disorder around the 16 position to which the nitroxide moiety is attached. One obtains the typical result that as the temperature increases the dynamics becomes faster, i.e. $\mathbf{R}$ increases; on the other hand the structure of the phase is almost the same because the order parameters hardly change.

One finds that the order parameter $\langle D^2_{00}\rangle$ obtained is essentially unchanged as a function of tilt angle $\mathbf{\Psi}$, as it should be. There is some variation in the optimum value of $R_\perp$, obtained as a function of tilt angle. An average over these values imparts an uncertainty of about 0.9% in log $R_\perp$ or about 17% in $R_\perp$. This uncertainty could be a measure of the limitation of the simple model in fitting the data (cf. below).

It should be noted that when the tilt angle is $\mathbf{\Psi} = 60°$ it is very close to the magic angle ($\mathbf{\Psi} = 54.736°$), which causes the function $\langle D^2_{00}\rangle(\mathbf{\Psi})$ in eq 12 to become very small. This fact makes this orientation rather insensitive to C_{20}. Thus the spectra for this orientation were fit with a C_{20} value which was the average obtained from the fits to the other angles.

3.3. Model B. In this model we did not consider the overall motion of the phospholipid molecule, i.e. we assumed this overall motion is slow enough to be in the rigid limit, and to take into account the range of orientations of the molecules in the vesicle we calculated a series of spectra for different orientations β of the lipid with respect to the director and then summed them with weights chosen according to the distribution given by eq 25. The free parameters of the model are the width of the distribution given by λ and the strength of the orienting interaction acting on each chain segment given by ϵ. In this case we did not use a least squares procedure to simulate the experimental spectra, but the free parameters of the model were adjusted by trial and error. The other parameters entering the calculation have been given the standard values:[8,9] $e_g = E_g/k_BT = 0.84$, $\rho = 1$, and $w = 5 \times 10^9$ s^{-1}. We obtained $\epsilon = 0.2$ and $\lambda = 20$.

Whereas the general shape of the spectra is reproduced, the line widths are too large because of the presence of the residual anisotropies of the magnetic interactions that are not averaged by the global motion of the phospholipid molecule.

3.4. Model C. The least squares fit procedure utilized for model A was modified to take into account the chain motions, as explained in section 2.2. The main changes were the use of a partially averaged magnetic tensor, calculated for given values of the parameter ϵ and expressing the strength of the orienting interaction, and the introduction of the angular-dependent T_2^{-1} of eq 15. The parameters that are fit are the same as for model A plus ϵ. However they have a different physical meaning. In model C the diffusion tensor refers only to the overall diffusive motion of the phospholipid molecule, which has the effect of averaging out the residual anisotropies left after the partial averaging from the internal motion of the chain. Analogously, the parameter C_{20} gives the strength of the orienting potential acting on the molecule as a whole, in addition to the potential acting on the individual segments. We have already discussed that the effect of the relatively fast motion of the chain is primarily to produce the partial averaging of the magnetic tensors. The line width contribution, given by eq 15 was found to make a negligible contribution for physically reasonable values of the motional parameters. That is, for $w \sim 5 \times 10^9$ s^{-1} the chain motions are fast enough to perform their partial averaging with only negligible residual line broadening.

The value of the ϵ parameter used for eq 26 is 0.5. This was obtained after some trial spectral fits. It was fixed for convenience during the least squares fits because the calculation of the full RIS model required is extremely time consuming. (Since there was little change in ordering with temperature (cf. below), ϵ was kept constant.) In this procedure, any changes in ordering would be reflected by changes in $\langle D^2_{00}\rangle$, which was not observed. The partially averaged magnetic tensors, reported in the appropriate principal axis system are

$$\bar{g}_{xx}, \bar{g}_{yy}, \bar{g}_{zz} = 2.0047, 2.0057, 2.0064$$

and

$$\bar{A}_{xx}, \bar{A}_{yy}, \bar{A}_{zz} = 11.9, 11.9, 18.3 \text{ G}$$

The Euler angles $\mathbf{\Phi} = (\alpha,\beta,\gamma)$ (cf. eq 2) representing the rotation from the diffusive system to the principal axis system of the $\bar{\mathbf{g}}$ tensor consist of $\alpha = 0°$, $\beta = 90°$, and $\gamma = -9.70°$. This represents the combined effect of averaging over the angles $\mathbf{\Omega}_4$, ω_1, ..., ω_{15}, and $\mathbf{\Omega}_5$ in eq 11. These coordinate systems

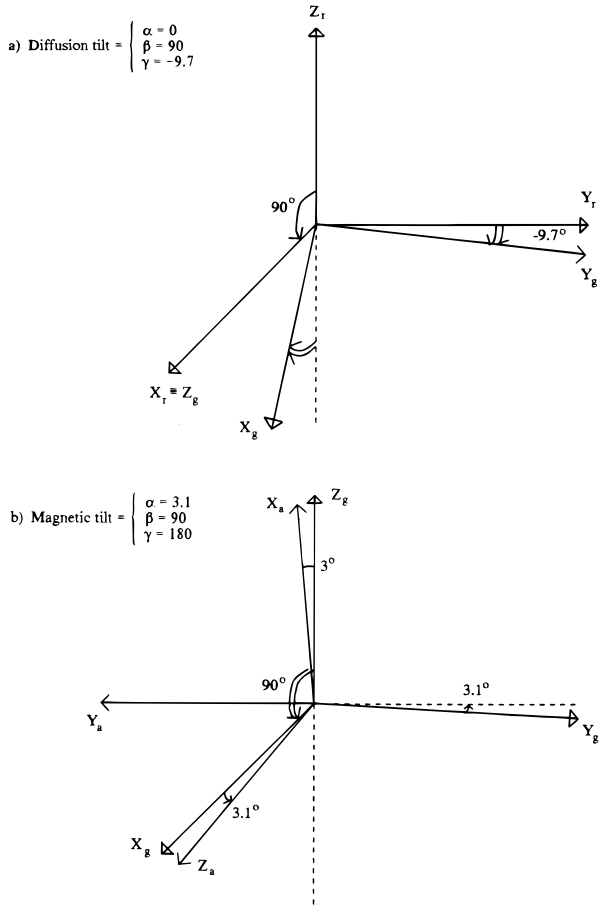

Figure 6. (a) Relation between principal axes for the diffusive system (X_R, Y_R, Z_R) and the partially averaged **g** tensor (X_g, Y_g, Z_g) and (b) relation between principal axes for the partially averaged **g** tensor (X_g, Y_g, Z_g) and the partially averaged **A** tensor (X_a, Y_a, Z_a).

and Euler angles are shown in Figure 6a. Note that the effective Z_g axis becomes parallel to the X_R axis for the rotational diffusion tensor, and the Y_g and X_g axes are rotated slightly (in the Y_R, Z_R plane) with respect to the Y_R and $-Z_R$ axes. Note also that the partially averaged **A** tensor axes are slightly tilted (by 3.1°) relative to the **g** tensor principal axes, with X_A, Y_A, and Z_A nearly parallel to Z_g, $-Y_g$, and X_g, respectively (cf. Figure 6b).

Table 2 reports the fitting parameters. The values of the diffusion tensor components, $R_\perp$ and $R_\parallel$, are substantially lower than those found using model A because in the present case they represent only the global motion of the phospholipid molecule. As in model A, C_{22} was set equal to zero in the simulation. Thus only the order parameter $\langle D^2_{00}\rangle$ is different from zero. It is higher than that for model A as expected because it is now indicative of the global alignment of the chains in the bilayer.

When we compare the quality of the fits in Figures 7 and 8 we see that the already rather good fits from model A are improved somewhat by model C, consistent with the reduced residuals to the fits. On the other hand there is somewhat more variation in $R_\perp$ obtained as a function of tilt angle Ψ. It is about double the variation in log $R_\perp$ for model C as compared to that for model A. Thus, while it appears that the partial averaging of the magnetic tensors due to the internal motions helps to improve the individual fits, the variation with Ψ in $R_\perp$ (and hence $R_\parallel$) would suggest some imperfections in precisely how this averaging has been performed. This is supported by the fact that this variation with Ψ is similar for the different temperatures. Cassol et al.[10] did find some differences in the averaging predicted by the RIS model vs what was calculated

TABLE 2: Best Fitting Parameters for the ESR Spectra of 16-PC in Aligned Membranes of DMPC Using Model C

T (°C)	log($R_\perp$)	log($R_\parallel$)	C_{20}	$\langle D^2_{00}\rangle$
		0° Tilt Angle		
35	7.00	7.58	1.87	0.41
40	7.15	7.70	1.73	0.38
45	7.27	7.80	1.73	0.38
50	7.34	7.89	1.65	0.37
55	7.38	7.94	1.74	0.39
60	7.50	8.03	1.70	0.38
65	7.54	8.06	1.75	0.39
		30° Tilt Angle		
35	7.20	7.80	1.88	0.41
40	7.31	7.91	1.81	0.40
45	7.41	8.01	1.74	0.39
50	7.46	8.06	1.70	0.38
55	7.51	8.11	1.70	0.38
60	7.58	8.18	1.75	0.39
65	7.61	8.21	1.68	0.37
		60° Tilt Angle		
35	7.15	7.75	1.90	0.42
40	7.25	7.85	1.81	0.40
45	7.34	7.94	1.73	0.38
50	7.41	8.01	1.69	0.38
55	7.38	7.98	1.69	0.38
60	7.60	8.20	1.71	0.38
65	7.64	8.24	1.66	0.37
		90° Tilt Angle		
35	6.68	7.28	1.94	0.43
40	6.94	7.54	1.89	0.42
45	7.13	7.73	1.73	0.38
50	7.20	7.80	1.73	0.38
55	7.29	7.89	1.61	0.36
60	7.37	7.97	1.68	0.37
65	7.44	8.04	1.54	0.34

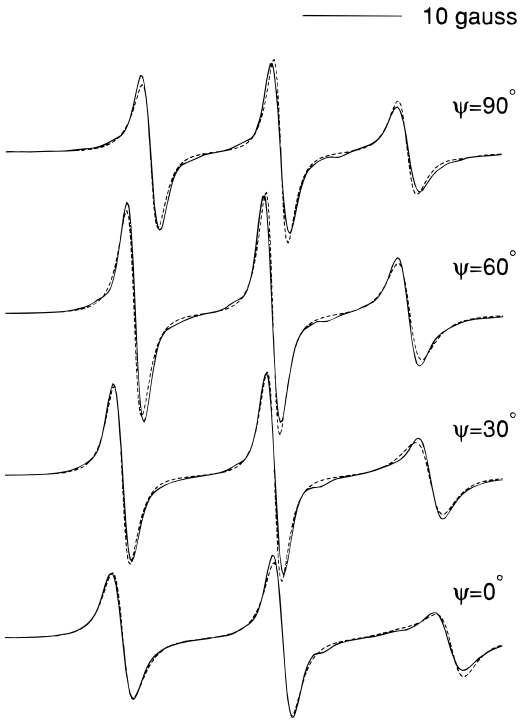

Figure 7. Comparison between best fits to model C (dashed lines) and experimental spectra (solid lines) obtained at 35 °C for the tilt angles shown.

with a Monte Carlo technique for an alkyl chain with eight rotating bonds. The longer chain in the present case does lead to the additional uncertainty in the RIS assumption of time scale separation between diffusive librations within the potential wells and the conformational transitions.[21] Also, we have included the role of the headgroup in an approximate manner. Addition-

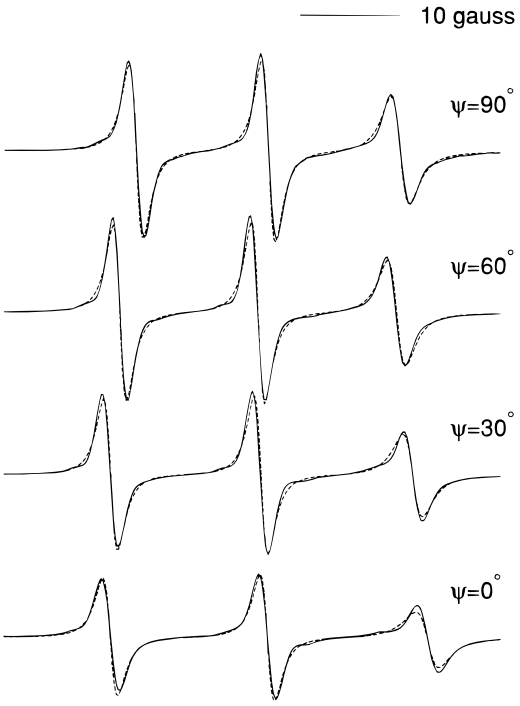

Figure 8. Comparison between best fits to model C (dashed lines) and experimental spectra (solid lines) obtained at 55 °C for the tilt angles shown.

ally we note that a mean field assumption has been made with respect to the interactions between chains. Any dynamic cooperativity has not been included in the model.

4. Summary

Our results show that model A based on the standard slow motional analysis and model C, which includes the chain dynamics, both give rather good fits to the experimental data on oriented membranes containing the 16-PC probe. This is because of the relative simplicity of the three line ESR spectra obtained. Thus, in the context of model A, the spectra are in the motional narrowing to incipient slow motional regime. Nevertheless, the results make clear the two differing viewpoints. In model A the parameters represent a composite effect from the chain dynamics and the overall motions. It shows the typical values of $R_\perp \approx 3-6 \times 10^8\ s^{-1}$ and low ordering $\langle D^2_{00}\rangle$ obtained previously.[5−7,11] Once the internal modes of motion are accounted for, as in model C, one finds that $R_\perp = 1-3 \times 10^7\ s^{-1}$ and $\langle D^2_{00}\rangle = 0.4$ which refer to just the overall motion of the lipid, and these values should be more realistic for this mode of motion as judged by the values found for a rigid spin-labeled cholesterol probe in lipid membranes.[6,7,11]

On the other hand, the experimental results and the comparisons with the two models do not enable one to rigorously test the model of the internal dynamic modes that is used. There are two directions that we propose in future work to obtain experimental results providing more resolution to the details of the modes of the chain dynamics. First of all, modern two-dimensional ESR methods have been found to be more sensitive to the details of the complex motions in related systems, e.g. liquid crystals containing spin probes.[22] Second, and perhaps even more important, should be complementary ESR studies at high fields and frequencies. High-frequency ESR has been shown to be particularly sensitive to complex motional dynamics.[23,24] In particular, one can predict that for ESR at 250 GHz, the modes of internal chain dynamics with a $w \sim 10^{10}\ s^{-1}$ will provide substantial broadening, i.e. they will not be too fast for these motions to be detected. On the other hand, values of $R_\perp = 1-3 \times 10^7\ s^{-1}$ are slow enough that the overall motion would be almost frozen out. Thus combined studies at 9.5 and 250 GHz could be expected to enable the two types of motion to be more clearly distinguished.

Acknowledgment. We thank Professor Pier-Luigi Nordio and Dr. Antonino Polimeno for helpful advice and encouragement. This work was supported by NIH Grant GM25862 and NSF Grant CHE 9313167.

References and Notes

(1) *Spin Labeling, Theory and Applications*; Berliner, L. J., Ed.; Academic Press: New York, 1976.
(2) *Biological Magnetic Resonance: Spin Labeling, Theory and Applications*; Berliner, L. J., Reuben, J., Eds.; Plenum: New York, 1989; Vol. 8.
(3) Schneider, D. J.; Freed, J. H. *Adv. Chem. Phys.* **1989**, *73*, 387.
(4) Schneider, D. J.; Freed, J. H. In *Spin Labeling Theory and Applications*; Berliner, L. J., Reuben, J., Eds.; Plenum: New York, 1989; Vol. 8, p 1.
(5) Ge, M.; Freed, J. H. *Biophys. J.* **1993**, *65*, 2106.
(6) Ge, M.; Budil, D. E.; Freed, J. H. *Biophys. J.* **1994**, *67*, 2326.
(7) Budil, D. E.; Lee, S.; Saxena, S.; Freed; J. H. *J. Magn. Res.* **1996**, *A120*, 155.
(8) Ferrarini, A.; Moro, G. J.; Nordio, P. L. *Mol. Phys.* **1988**, *63*, 225. Moro, G. J.; Ferrarini, A.; Polimeno, A.; Nordio, P. L. In *Reactive and Flexible Molecules in Liquids*; Dorfmüller, Th., Ed.; Kluwer Academic: Dordrecht, The Netherlands, 1988.
(9) Ferrarini, A.; Nordio, P. L.; Moro, G. J.; Crepeau, R. H.; Freed, J. H. *J. Chem. Phys.* **1989**, *91*, 5707.
(10) Cassol, R.; Ferrarini, A.; Nordio, P. L. *J. Phys. Chem.* **1993**, *97*, 2933−2940.
(11) Shin, Y. K.; Budil, D. E.; Freed, J. H. *Biophys. J.* **1993**, *65*, 1283.
(12) Flory, P. J. *Statistical Mechanics of Chain Molecules*; Interscience: New York, 1969.
(13) Redfield, A. G. *Adv. Magn. Reson.* **1965**, *1*, 1.
(14) Freed, J. H., Fraenkel, G. K. *J. Chem. Phys.* **1963**, *39*, 326.
(15) Freed, J. H.; Nayeem, A.; Rananavare, S. B. In *The Molecular Dynamics of Liquid Crystals*; Luckhurst, G. R., Veracini, C. A., Eds.; Kluwer: Dordrecht, The Netherlands, 1994; Chapter 12.
(16) Marcelja, S. *Biochim. Biophys. Acta* **1974**, *367*, 165; *Nature* **1973**, *241*, 451.
(17) Kramers, H. A. *Physica* **1940**, *7*, 284.
(18) Langer, J. S. *Ann. Phys.* **1969**, *54*, 258.
(19) Ge, M.; Freed, J. H. *Biophys. J.*, in press.
(20) Our procedure here is somewhat different from that recommended by Budil et al.[7] These authors properly recommend that one simultaneously fit the spectra at all tilt angles, **Ψ**, in order to obtain the best fitting parameters to a given model. Our purpose in the present work is a little different in that we wanted to evaluate the quality of fit of the respective models, and we found it useful to follow the trends in the fits with **Ψ**. The extent to which the optimum values of a parameter such as $R_\perp$ varies with **Ψ** is useful for such a comparison, as we discuss in the text.
(21) Moro, G. J. *J. Chem. Phys.* **1991**, *94*, 8577. Cassol, R.; Ferrarini, A.; Nordio, P. L. *J. Phys.: Condens. Matter* **1994**, *6*, A279.
(22) Sastry, V. S. S.; Polimeno, A.; Crepeau, R. H.; Freed, J. H. *J. Chem. Phys.* **1996**, *105*, 5753; 5773.
(23) Polimeno, A.; Freed, J. H. *J. Phys. Chem.* **1995**, *99*, 10995.
(24) Earle, K. A.; Mocischi, J. K.; Polimeno, A.; Freed, J. H. *J. Chem. Phys.* **1997**, *106*, 9996.